



PCCP

Predictions of Delafossite-Hosted Honeycomb and Kagome Phases

Journal:	<i>Physical Chemistry Chemical Physics</i>
Manuscript ID	CP-ART-08-2023-004039.R1
Article Type:	Paper
Date Submitted by the Author:	22-Dec-2023
Complete List of Authors:	Krogel, Jaron; Oak Ridge National Laboratory, Materials Science and Technology Division Ichibha, Tom; Oak Ridge National Laboratory, Materials Science and Technology Division Saritas, Kayahan; Oak Ridge National Laboratory, Materials Science and Technology Division Yoon, Mina; Oak Ridge National Laboratory Reboredo, Fernando ; Oak Ridge National Laboratory, Materials Science & Technology Division

SCHOLARONE™
Manuscripts

Predictions of Delafossite-Hosted Honeycomb and Kagome Phases

Jaron T. Krogel,¹ Tomohiro Ichibha,¹ Kayahan Saritas,¹ Mina Yoon,¹ and Fernando A. Reboredo¹
Materials Science and Technology Division, Oak Ridge National Laboratory, Oak Ridge, TN 37831, USA

(Dated: 5 February 2024)

Delafossites, typically denoted by the formula ABO_2 , are a class of layered materials that exhibit a wide range of electronic and optical properties. Recently, the idea of modifying these delafossites into ordered kagome or honeycomb phases via strategic doping has emerged as a potential way to tailor these properties. In this study, we use high-throughput density functional theory calculations to explore many possible candidate kagome and honeycomb phases by considering dopants selected from the parent compounds of known ternary delafossite oxides from the Inorganic Crystal Structure Database. Our results indicate that while A-site in existing delafossites can host a limited range of elemental species, and display a low propensity for mixing or ordering, the oxide sub-units in the BO_2 much more readily admit guest species. Our study identifies four candidate B-site kagome and fifteen candidate B-site honeycombs with a formation energy more than 50 meV/f.u. below other competing phases. The ability to predict and control the formation of these unique structures offers exciting opportunities in materials design, where innovative properties can be engineered through the selection of specific dopants. A number of these constitute novel correlated metals, which may be of interest for subsequent efforts in synthesis. These novel correlated metals may have significant implications for quantum computing, spintronics, and high-temperature superconductivity, thus inspiring future experimental synthesis and characterization of these proposed materials.

1

I. INTRODUCTION

The computational design of materials with targeted properties and functionalities has been a long standing and ambitious motivation for improving the speed and accuracy of theoretical methods in materials along many decades. In a data driven approach a massive number of existing structures are explored with alternative atomic compositions. Subsequently, the data set of the structures studied theoretically, is searched to find the best properties. While experimental exploration always remains a crucial step, theory can be still highly valuable removing structures and compositions which are found to be thermodynamically unstable. In addition, theory can be used to screen out the ones without desired properties and reduce further the exploration to a smaller number that must be finally explored experimentally.

Topological materials^{1–3}, characterized by unique electronic properties, are emerging as promising candidates for future quantum technologies due to their robustness

to local perturbations. The study of specific lattice structures is crucial to reveal the different topological phases of these materials. The honeycomb lattice, as found in graphene, exhibits intriguing phenomena due to the presence of two-dimensional Dirac cones. When manipulated by spin-orbit coupling, these cones can promote topologically protected edge states, creating a fertile ground for the study of topological insulators⁴. On the other hand, the kagome lattice forms a network of corner-sharing triangles and is known to host exotic phenomena due to its inherent geometric frustration. The potential hosting of localized, topologically distinct electronic bands, known as flat bands, in kagome lattices provides an exciting avenue for the study of strongly correlated topological phases of matter⁵. Thus, the unique geometries and quantum mechanical effects within these lattices provide an opportunity to observe unusual and exotic electronic behaviors, highlighting the importance of honeycomb and kagome lattices in topological materials research.

Delafossite compounds^{6,7} are naturally occurring minerals with a layered structure that is of particular interest to physicists and materials scientists. Their crystal structure forms a triangular lattice, which is one of the simplest two-dimensional geometries. Triangular lattices are, in many ways, the starting point for other two-dimensional structures, such as the honeycomb and kagome lattices. Recently, it has been proposed⁸ to modify delafossites (ABO_2) to adopt ordered binary intralayer patterns that might host phases with non-trivial topology, such as the honeycomb or kagome quasi-2D lattices. This approach is promising, since several ternary delafossite-like compounds that host honeycomb order on the B-site sub-lattice ($\text{AB}_{2/3}\text{B}'_{1/3}\text{O}_2$) are known to exist^{9–19} for both the dumbbell/linear coordinated and rocksalt type structures. We are interested in finding

¹ This manuscript has been authored by UT-Battelle, LLC under Contract No. DE-AC05-00OR22725 with the U.S. Department of Energy. The United States Government retains and the publisher, by accepting the article for publication, acknowledges that the United States Government retains a non-exclusive, paid-up, irrevocable, worldwide license to publish or reproduce the published form of this manuscript, or allow others to do so, for United States Government purposes. The Department of Energy will provide public access to these results of federally sponsored research in accordance with the DOE Public Access Plan (<http://energy.gov/downloads/doe-public-access-plan>).

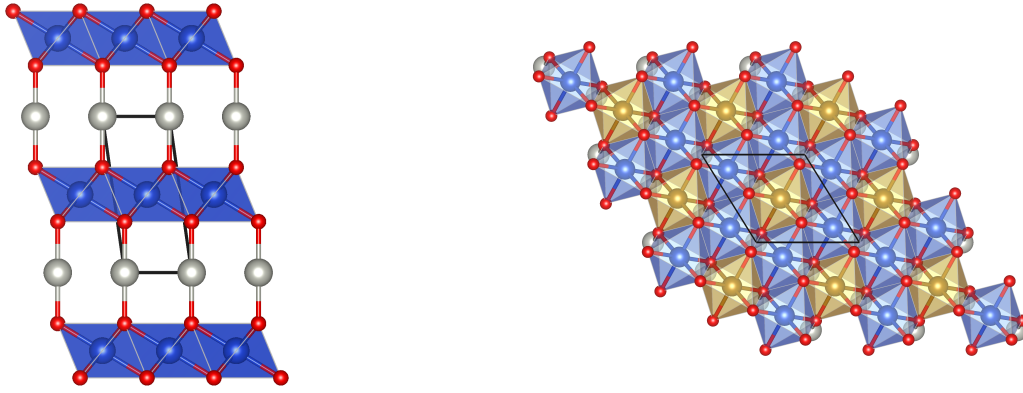


FIG. 1. The “dumbbell” type delafossite ABO_2 structure (left). Oxide layers composed of BO_2 octahedra are separated by triangular A layers with A-site atoms aligned linearly with neighboring oxygen. (right) Top view of the $B_{2/3}B'_{1/3}O_2$ layer in a B-site honeycomb ordered quaternary delafossite-like crystal.

the material combinations in which a kagome lattice or a honeycomb lattice can self-assemble.

In this work, we perform a data-driven approach to ascertain suitable dopants in existing delafossites that would preferentially order into kagome or honeycomb lattices instead of segregating in separate triangular phases. This procedure allows us to discard a large number of material combinations in which the honeycomb or the kagome lattice is thermodynamically unstable. We also identify in our search a set of new delafossites that are predicted to be stable within a standard approximation of density functional theory^{20,21} (DFT).

II. METHODS

In order to identify candidate ternary structures, we considered as potential parent compounds 55 known ternary delafossite oxide structures from the Inorganic Crystal Structure Database (ICSD)²². Among these, 26 displayed the dumbbell-like bonding arrangement on the A-site (see Fig. 1), while 29 instead adopted an ordered rocksalt structure. Both structure types share the same space-group ($R\bar{3}m$) and differ primarily in the Wyckoff position of the oxygen sub-lattice, with dumbbell bonded and ordered rocksalt crystals having a Wyckoff parameter near 0.11 and 0.25, respectively. For some selections of A and B elements these two types of local order can compete, with crystals hosting both types of local order being reported in different layers along the c-axis²³.

From these parent ABO_2 structures, we formed hypothetical A and B site-ordered honeycomb and kagome quaternary materials of the form $A_{1-x}A'_xBO_2$ and $AB_{1-x}B'_xO_2$ ($x = 1/3$ for honeycomb and $x = 1/4$ for kagome, see Fig. 1). To limit the search to a practical number, instead of studying all stable elements in the periodic table, we down-selected the impurities with the following criterion. Since the set of A and B elements in the parent compounds are already known to support the local bonding arrangements expected in delafossites, we

restricted the A' and B' elements to be selected from this same set. Under this restricted search, 2592 quaternary ordered phases were considered.

Each of the quaternary candidate structures was fully relaxed within at the PBE²⁴/PBE+U²⁵ level of theory. The candidate structures were subsequently screened for stability by considering the ground state energy convex hull of competitive compounds. These stability calculations included the total energies E_i of (i) elemental solids, (ii) low energy binary oxides (selected from the Materials Project²⁶ with the search criteria of having above hull energies being less than 0.1 eV/atom), (iii) known delafossites, and (iv) hypothetical delafossites with composition $A'BO_2$ or $AB'O_2$ (as these provide an additional bound on the formation of the quaternary cases).

The lowest energy mixture of phases at a given composition (convex hull) was found by minimizing the relation

$$E(f) = \min_c \sum_i c_i E_i \quad (1)$$

subject to the constraints

$$c_i \geq 0 \quad , \quad Nc = f. \quad (2)$$

In the expressions above, f represents the target composition as a vector of atomic fractions, N is a matrix containing the atomic fractions for each computed compound (N_i is a vector of atomic fractions for compound i), E_i is the total energy of each respective compound, and c_i is the concentration of each compound present in the final lowest energy mixture of phases. The (minimum) formation energy of compound j is defined here as

$$E_{F,j} = E_j - E(N_j) \quad (3)$$

with the minimization in Eq. 1 excluding compound j itself. If $E_F < 0$ the compound is stable against all alternatives included in Eq. (1). Conversely, if $E_F > 0$ the compound is unstable.

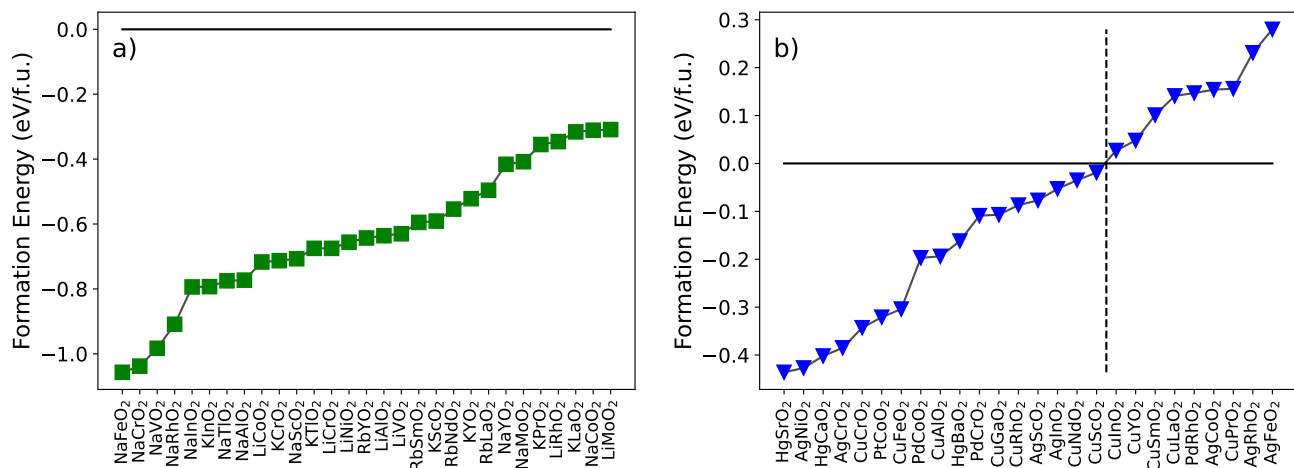


FIG. 2. Calculated formation energies per formula unit (eV/f.u.) of a) ordered rocksalt type and b) dumbbell type delafossite compounds selected from ICSD. The connecting line is a guide to the eye. The formation energies are computed relative to competing elemental and binary oxide phases.

The stability of rocksalt and dumbbell delafossites was assessed relative to decomposition into binary and elemental phases (see Figs. 2 and 3). When considering the propensity for a given site (A or B) to accept dopant species (4), the formation energies are also computed relative to decomposition into lower order phases (elemental solids, binary oxides, ternary delafossites). The final assessment of stable honeycomb and kagome phases (see Table I) is performed including the possibility for the dopant to occupy either site (all quaternary mixed delafossites included as competitor phases in addition to other lower order phases).

The total energies of all phases were computed with the PBE functional²⁴ as implemented in the VASP package version 5.4.4^{27–30}. For transition metal elements, a Hubbard U was added to represent the on-site Coulomb repulsion among the localized d -electrons²⁵. In high throughput studies, the Hubbard U parameter is often either neglected^{31–33}, set to a single value for all species^{34,35}, or set to unique values per element^{36,37} (often selected semi-empirically) and then held fixed across compounds. We follow the former approach. In diffusion Monte Carlo calculations of correlated oxides, a U value between 2 and 6 eV is often found^{38–51} with a value near 3 eV occurring most often, and so we selected $U=3.0$ eV in all calculations. In SCF and structural relaxation calculations a k -point grid of $13 \times 13 \times 13$ per ABO_2 primitive cell (or finer) was used and relaxed structures were obtained with 10^{-6} eV and 0.01 eV/Å tolerances on the total energy and maximum atomic force, respectively. For the correlated oxides, the Hubbard U was applied consistently to both the structural relaxation and subsequent SCF calculations. While the present study focuses on materials stability, band gap information for parent delafossites may be found in the supplementary information. For more detailed information on band gaps in the delafossites, the

interested reader is referred to prior theory work⁵² in this area.

III. RESULTS AND DISCUSSION

A. Formation energies of known delafossites

The calculated formation energies of synthesized delafossites are shown in Fig. 2. The formation energies are computed relative to competing elemental and binary oxide phases. All of the rock-salt type delafossites (left panel) are validated as being stable with large formation energies. The unusual linear bonding arrangement of the A-site in the dumb-bell type delafossites (typically $A^{1+}B^{3+}$) and the noble or near noble quality⁵³ of the known A-site elements results in a lower formation energy for this class of delafossites, as shown in the right panel of Fig. 2. While most of the synthesized delafossites are predicted to be stable by these total energy calculations, a significant fraction is not. A closer comparison with the experimental literature shows some of these predictions to be correct. In particular, $CuLaO_2$ is known to be unstable to O_2 exposure at temperatures as low as $280^\circ C$ with ready oxidation also being observed for other lanthanides on the B-site⁵⁴, as well as for the chemically similar $CuYO_2$ ⁵⁵. The $CuInO_2$ is also very difficult to synthesize and is assessed to be metastable relative to other end-member phases⁵⁶. The predicted instability of $PdRhO_2$ and three of the $AgMO_2$ phases is incorrect and may relate to the limitations intrinsic to the approximate density functional employed here.

B. Predicted low formation energy delafossites

As part of the search for ordered ternary delafossite-like oxides, formation energies for large number of possible end-member delafossites with composition $A'BO_2$ and $AB'O_2$ were calculated. Among these, a small number were shown to be stable against decomposition into binary oxides and elemental solids. The formation energies of the predicted stable delafossites is shown in Fig. 3, where we have used a formation energy of 50 meV/f.u. as a threshold for inclusion.

Among these, a deeper review of the available literature shows that about half of the predicted stable delafossites are known to form already, with some being synthesized only recently. The Ag-based compounds, $AgAlO_2$ and $AgGaO_2$ are commonly grown^{6,57}, but were not selected as part of our initial search of the ICSD. The Cu containing delafossites $CuVO_2$ and $CuNiO_2$ were thought not to exist⁵⁸, but thin films of $CuNiO_2$ have been successfully grown via the sol gel technique⁵⁹ and nanoplate samples of $CuVO_2$ have recently been obtained by hydrothermal synthesis⁶⁰. Finally, while few Pt-based delafossites are commonly known to exist^{6,61}, a recent thermal decomposition study⁶² of Pt and Pd complex salts of the form $[M(NH_3)_4]CrO_4$ ($M=Pt,Pd$) has shown the presence of both $PdCrO_2$ and $PtCrO_2$ phases via XRD in narrow temperature range around 700 °C.

Out of the predicted stable delafossites, four are metals: $PdAlO_2$, $PdNiO_2$, $PtCrO_2$, and $PtNiO_2$. These phases are of particular interest due to the record high mobilities observed in related compounds such as $PdCoO_2$. The Cr and Ni containing compounds might also host Kondo type physics due to the interaction between delocalized A-site carriers and localized magnetic states on the B-sublattice. Recently, $PtNiO_2$ has been predicted to host a topological Weyl metal phase⁶³ and its stability has also been suggested by another high-throughput *ab initio* study⁶⁴.

C. Predictions related to miscibility

The formation energies of the quaternary candidate phases with mixed A or B site composition computed relative to the lower order (ternary and below) phases contains information about the propensity for intralayer mixing. In this setting, a negative formation energy indicates favorable conditions for mixing in general, since the energies of the currently considered ordered candidate structures constitute upper bounds on all other ordered or disordered structures at the same composition.

In Fig. 4 we organize the formation energies of all 2592 calculated ordered honeycomb/kagome candidate structures organized by parent phase. Mixing on the A and B sites are considered separately in Figs. 4a and 4b, respectively, and formation energies larger than 0.25 eV are excluded from the plots. For the case of A-site mixing, nearly all of the considered candidate mixtures have pos-

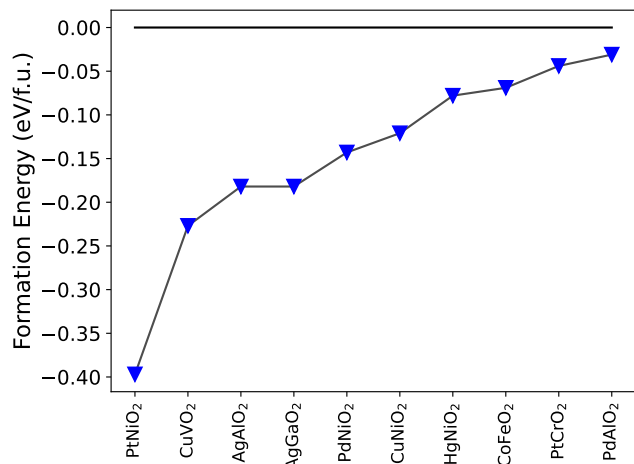


FIG. 3. Predicted delafossite compounds (dumbbell ABO_2) identified as theoretically stable, within the PBE+U approximation, during the high-throughput search. The blue line is a guide to the eye. Stability is indicated by negative formation energies (eV/f.u.) relative to competing elemental and binary oxide phases.

itive formation energies and thus mixing on the A-site is largely disfavored for the considered ordered structures. Therefore, unless other ordered structures have significantly lower formation energy than those considered here, realized A-site site mixtures are likely to be disordered. Further, the majority of favorable A-site mixtures have a very low formation energy, which implies easy decomposition into competing disordered or lower order ordered phases upon heating. Taken together, these results indicate that delafossite-like structures with A-site honeycomb or kagome intermetallic order are quite rare if they do exist and are unlikely to be synthesized via trial and error.

In contrast to the A-site, mixing on the B-site is favored for a much larger range of compounds. Therefore facile mixing is not uncommon on the B-site of delafossites. However, the propensity for parent delafossites to host mixed phases is not uniform, with certain ABO_2 compounds having the ability to admit many different dopant species. In particular, $AgNiO_2$ and $AgFeO_2$ are predicted to readily form B-site mixtures. The parent delafossites identified here as readily hosting guest species may be useful as a starting point for a more in depth search for ordered B-site phases involving a larger number of candidate guest elements. We also note that since the ordered structures considered here have low formation energy on the B-site, the existence of some ordered phases involving mixture on this site are more likely. This assessment is also verified experimentally, as it is consistent with the observation of several ordered B-site honeycomb phases^{10–19}.

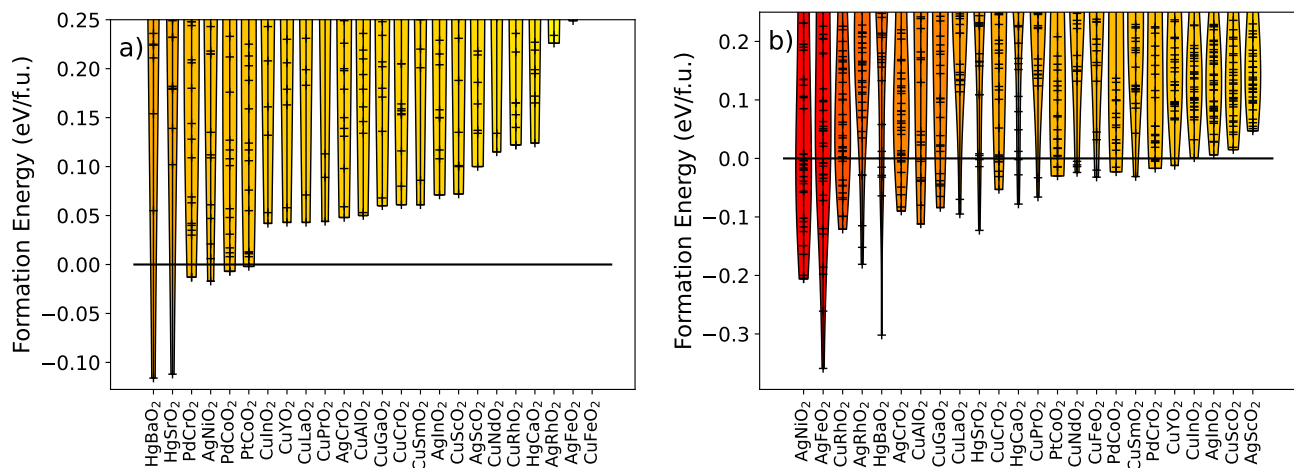


FIG. 4. Propensity for intra-layer doping/mixing as indicated by formation energies of quaternary mixed delafossites with ordered kagome or honeycomb phases arranged on a) the A-site ($A_{1-x}A'_xBO_2$) or b) the B-site ($AB_{1-x}B'_xO_2$). Each horizontal bar represents the formation energy of a distinct honeycomb or kagome compound. The formation energies (eV/f.u. ABO_2) are assessed relative to lower order phases (elemental solids, binary oxides, and ternary ABO_2 phases). The labeled phase denotes the parent/host ABO_2 and the color of each column relates to the overall miscibility of the host, with red indicating a larger number of miscible dopants.

D. Candidate A-site ordered delafossite-like compounds

In a recent dynamical mean field theory (DMFT) work⁸, interest was raised in the possibility of A-site ordered delafossite phases. Here we evaluate possible kagome (KG - $A_{3/4}A'_{1/4}BO_2$) or honeycomb (HC - $A_{2/3}A'_{1/3}BO_2$) ordered lattices on the A-site in terms of their energetic favorability. This favorability is assessed in terms of the formation energy of a particular proposed KG or HC phase against elemental solids, binary oxides, ternary rocksalt and dumbbell delafossites, and also against the other possible quaternary ordered HC/KG phases on the A or B site.

On the A-site, we do not find any significant evidence for honeycomb ordering, with all AA' pairings resulting in formation energies above -20 meV/f.u.. We also find that candidates for A-site kagome order are very rare. Out of the entire search space, we find only two candidates: $Hg_{3/4}Cu_{1/4}SrO_2$ and $Hg_{3/4}Li_{1/4}BaO_2$ (see Table I). These related structures are favored over the parent delafossites ($HgSrO_2$ and $HgBaO_2$) as well as nearby B-site ordered competitor phases by about 100 meV. The acceptable introduction of Cu may be rationalized by the common 2^+ oxidation state of Cu, similar to Hg and Sr themselves. The uptake of Li is less intuitive, but may relate to facile electron donation from Li as compared to Hg to stabilize the BaO_2 unit, which also can exist as a stable oxide in isolation⁶⁵. All other structures with close to zero formation energy involve either mixtures of known A-site species for the dumbbell delafossites (Cu, Ag, Pd, Pt, Hg) or the A-site pairing of Cu (majority) and Li (minority) combined either with indium or group III elements (including lanthanides) on the B-site.

E. Candidate B-site ordered delafossite-like compounds

The search for B-site ordering in delafossites is conceptually similar to the cation ordering in layered cathodes where multiple cations are combined to improve its cyclic properties⁶⁶. Compared to cathode materials, however, long-range kagome and honeycomb ordering in delafossites place more stringent criteria in our materials search. Identified candidates are summarized in Table I. Our search yields only a few kagome ordered delafossites with $AgFeO_2$ and $AgNiO_2$ parent compounds with Ca, Ni, Al and Mo dopants. Experimentally, the only B-site kagome ordered delafossite derived compounds found are hole-doped with cation deficiencies, $YCuO_{2.5}$ ⁵⁵ and $LaCuO_{2.5}$ ⁵⁴. However, our search has predicted a larger set of honeycomb ordered B-site delafossites, that is consistent with the large number of experimentally observed honeycomb ordered B-site delafossites⁹⁻¹⁹.

Stable B-site honeycombs can be divided into multiple groups with common oxidation states such as $Hg^{1+}\{Ca, Sr, Ba\}_{2/3}Mo_{1/3}^{5+}O_2$, $Ag^{1+}Fe_{2/3}^{3.5+}\{Ba, Sr\}_{1/3}^{2+}O_2$ and $Ag^{1+}\{Rh, Fe, Ni, Cr\}_{2/3}^{4+}\{Li, Na\}_{1/3}^{1+}O_2$. Except for the $Hg^{1+}\{Ca, Sr, Ba\}_{2/3}Mo_{1/3}^{5+}O_2$ group, it is a common feature that the base B-site atom has close to 4^+ formal oxidation state. Among these compounds, $AgRh_{2/3}Li_{1/3}O_2$ has been synthesized experimentally demonstrating long range ordering of honeycomb lattice¹⁵. However, it can be argued that 4^+ is not a common oxidation state for Fe, Ni, Cr in their respective compounds. Nevertheless, these B-site ordered delafossites have metallic band structures that can accommodate deviations from a simple valence assignments, such as hole formation on O- p states could occur. Un-

less the experimental synthesis conditions are carefully tailored, it is possible that oxygen vacancies can form with negative formation energies similar to the Y- and LaCuO_{2.5}^{54,55}. Therefore, further investigations may be needed to understand if oxygen vacancies would form in an ordered way in the proposed structures to preserve their honeycomb lattice ordering.

A-site Kagome	E_F (meV/f.u.)
Hg _{3/4} Cu _{1/4} SrO ₂	-112
Hg _{3/4} Li _{1/4} BaO ₂	-98
B-site Kagome	E_F (meV/f.u.)
AgFe _{3/4} Ni _{1/4} O ₂	-215
AgFe _{3/4} Ca _{1/4} O ₂	-129
AgNi _{3/4} Mo _{1/4} O ₂	-128
AgFe _{3/4} Al _{1/4} O ₂	-072
B-site Honeycomb	E_F (meV/f.u.)
HgBa _{2/3} Mo _{1/3} O ₂	-274
AgFe _{2/3} Li _{1/3} O ₂	-207
AgFe _{2/3} Sr _{1/3} O ₂	-198
AgRh _{2/3} Na _{1/3} O ₂	-133
HgSr _{2/3} Mo _{1/3} O ₂	-123
AgFe _{2/3} Na _{1/3} O ₂	-120
AgNi _{2/3} Li _{1/3} O ₂	-104
AgRh _{2/3} Li _{1/3} O ₂	-98
HgCa _{2/3} Mo _{1/3} O ₂	-78
AgNi _{2/3} Pd _{1/3} O ₂	-67
AgCr _{2/3} Li _{1/3} O ₂	-67
AgFe _{2/3} Ba _{1/3} O ₂	-63
CuLa _{2/3} Pr _{1/3} O ₂	-62
AgNi _{2/3} Pt _{1/3} O ₂	-60
CuLa _{2/3} Nd _{1/3} O ₂	-59

TABLE I. A-site and B-site kagome and honeycomb structures identified as stable during the high-throughput search. The formation energies are computed relative to competing elemental solids, binary oxides, ternary delafossites, and other quaternary mixed delafossites (including mixing on both A and B sites).

IV. CONCLUSION

We have performed a high-throughput search for candidate honeycomb and kagome delafossite derived crystal phases based on *ab initio* density functional theory calculations within the PBE+U approximation. Our data-driven materials discovery approach was validated against the stability of known delafossites and generally showed good agreement with current experimental knowledge of these phases. We found that the miscibility of parent delafossites depends strongly on the site of the introduced guest species. In particular, we found only two thermodynamically stable structures involving mixing on the A-site. In contrast, we find ready mixing on the B-site with 15 candidate B-site honeycomb and 4 candidate B-site kagome phases with stability greater than 50 meV identified from the high-throughput search. One

of the identified phases, AgRh_{2/3}Li_{1/3}O₂, has been synthesized already and we may expect others of the identified ordered structures to also be synthesizable. A key consideration in this regard is the stability of the candidate phases to lattice disorder. This topic will be the subject of future work.

V. ACKNOWLEDGEMENTS

The authors would like to thank Markus Eisenbach for useful discussions and for providing a thorough reading of the manuscript. This work was supported by the U.S. Department of Energy, Office of Science, Basic Energy Sciences, Materials Sciences and Engineering Division. This research used resources of the Compute and Data Environment for Science (CADES) at the Oak Ridge National Laboratory, which is supported by the Office of Science of the U.S. Department of Energy under Contract No. DE-AC05-00OR22725. This research also used resources of the Research Center for Advanced Computing Infrastructure (RCACI) at JAIST.

- ¹M. Z. Hasan and C. L. Kane, *Rev. Mod. Phys.*, 2010, **82**, 3045–3067.
- ²X.-L. Qi and S.-C. Zhang, *Rev. Mod. Phys.*, 2011, **83**, 1057–1110.
- ³B. A. Bernevig, C. Felser and H. Beidenkopf, *Nature*, 2022, **603**, 41–51.
- ⁴K.-H. Jin and S.-H. Jhi, *Phys. Rev. B*, 2013, **87**, 075442.
- ⁵J.-X. Yin, B. Lian and M. Z. Hasan, *Nature*, 2022, **612**, 647–657.
- ⁶R. D. Shannon, D. B. Rogers and C. T. Prewitt, *Inorganic Chemistry*, 1971, **10**, 713–718.
- ⁷M. A. Marquardt, N. A. Ashmore and D. P. Cann, *Thin Solid Films*, 2006, **496**, 146–156.
- ⁸F. Lechermann, *npj Computational Materials*, 2021, **7**, 120.
- ⁹R. Nagarajan, S. Uma, M. Jayaraj, J. Tate and A. Sleight, *Solid State Sciences*, 2002, **4**, 787–792.
- ¹⁰R. Berthelot, W. Schmidt, S. Muir, J. Eilertsen, L. Etienne, A. W. Sleight and M. A. Subramanian, *Inorganic Chemistry*, 2012, **51**, 5377–5385.
- ¹¹E. A. Zvereva, M. I. Stratan, A. V. Ushakov, V. B. Nalbandyan, I. L. Shukaev, A. V. Silhanek, M. Abdel-Hafiez, S. V. Streltsov and A. N. Vasiliev, *Dalton Trans.*, 2016, **45**, 7373–7384.
- ¹²E. A. Zvereva, M. I. Stratan, A. V. Ushakov, V. B. Nalbandyan, I. L. Shukaev, A. V. Silhanek, M. Abdel-Hafiez, S. V. Streltsov and A. N. Vasiliev, *Dalton Trans.*, 2016, **45**, 7373–7384.
- ¹³M. Abramchuk, O. I. Lebedev, O. Hellman, F. Bahrami, N. E. Mordvinova, J. W. Krizan, K. R. Metz, D. Broido and F. Tafti, *Inorganic Chemistry*, 2018, **57**, 12709–12717.
- ¹⁴S. Bette, T. Takayama, V. Duppel, A. Poulain, H. Takagi and R. E. Dinnebier, *Dalton Trans.*, 2019, **48**, 9250–9259.
- ¹⁵R. Kumar, T. Dey, P. M. Ette, K. Ramesha, A. Chakraborty, I. Dasgupta, R. Eremina, S. Tóth, A. Shahee, S. Kundu, M. Prinz-Zwick, A. A. Gippius, H. A. K. von Nidda, N. Büttgen, P. Gegenwart and A. V. Mahajan, *Phys. Rev. B*, 2019, **99**, 144429.
- ¹⁶D. K. Yadav, A. Sethi, Shalu and S. Uma, *Dalton Trans.*, 2019, **48**, 8955–8965.
- ¹⁷B. Huang, Z. Liu, Y. Han, S. Zhao, M. Wu, C. E. Frank, M. Greenblatt, M. Croft, N. F. Quackenbush, S. Liu, T. A. Tyson, L. Zhang, J. Sun, P. Shan, J. Dai, X. Yu, J. Cheng and M.-R. Li, *Chem. Commun.*, 2020, **56**, 265–268.
- ¹⁸A. Karati, T. Parida, J. Gupta, H. K. Adigilli, P. H. Borse and J. Joardar, *Materials Research Bulletin*, 2021, **137**, 111181.
- ¹⁹J. H. Roudebush, K. A. Ross and R. J. Cava, *Dalton Trans.*, 2016, **45**, 8783–8789.

- ²⁰P. Hohenberg and W. Kohn, *Phys. Rev.*, 1964, **136**, B864.
- ²¹W. Kohn and L. Sham, *Phys. Rev.*, 1965, **140**, A1133–A1138.
- ²²M. Hellenbrandt, *Crystallography Reviews*, 2004, **10**, 17–22.
- ²³R. Berthelot, M. Pollet, J.-P. Doumerc and C. Delmas, *Inorganic Chemistry*, 2011, **50**, 6649–6655.
- ²⁴J. P. Perdew, K. Burke and M. Ernzerhof, *Phys. Rev. Lett.*, 1996, **77**, 3865.
- ²⁵V. Anisimov, J. Zaanen and O. Andersen, *Physical Review B*, 1991, **44**, 943.
- ²⁶A. Jain, S. P. Ong, G. Hautier, W. Chen, W. D. Richards, S. Dacek, S. Cholia, D. Gunter, D. Skinner, G. Ceder and K. A. Persson, *APL Materials*, 2013, **1**, year.
- ²⁷G. Kresse and J. Hafner, *Phys. Rev. B*, 1993, **47**, 558–561.
- ²⁸G. Kresse and J. Furthmüller, *Computational Materials Science*, 1996, **6**, 15–50.
- ²⁹G. Kresse and J. Furthmüller, *Phys. Rev. B*, 1996, **54**, 11169–11186.
- ³⁰G. Kresse and D. Joubert, *Phys. Rev. B*, 1999, **59**, 1758–1775.
- ³¹K. Choudhary, I. Kalish, R. Beams and F. Tavazza, *Scientific Reports*, 2017, **7**, 5179.
- ³²J. Balluff, K. Diekmann, G. Reiss and M. Meinert, *Phys. Rev. Mater.*, 2017, **1**, 034404.
- ³³D. Broberg, K. Bystrom, S. Srivastava, D. Dahliah, B. A. D. Williamson, L. Weston, D. O. Scanlon, G.-M. Rignanese, S. Dwaraknath, J. Varley, K. A. Persson, M. Asta and G. Hautier, *npj Computational Materials*, 2023, **9**, 72.
- ³⁴X. Li, Z. Zhang and H. Zhang, *Nanoscale Adv.*, 2020, **2**, 495–501.
- ³⁵B. Baldassarri, J. He, X. Qian, E. Mastronardo, S. Griesemer, S. M. Haile and C. Wolverton, *Phys. Rev. Mater.*, 2023, **7**, 065403.
- ³⁶W. Setyawan, R. M. Gaume, S. Lam, R. S. Feigelson and S. Curtarolo, *ACS Combinatorial Science*, 2011, **13**, 382–390.
- ³⁷M. K. Horton, J. H. Montoya, M. Liu and K. A. Persson, *npj Computational Materials*, 2019, **5**, 64.
- ³⁸K. Foyevtsova, J. T. Krogel, J. Kim, P. R. C. Kent, E. Dagotto and F. A. Reboredo, *Phys. Rev. X*, 2014, **4**, 031003.
- ³⁹A. Benali, L. Shulenburg, J. T. Krogel, X. Zhong, P. R. C. Kent and O. Heinonen, *Phys. Chem. Chem. Phys.*, 2016, **18**, 18323–18335.
- ⁴⁰Y. Luo, A. Benali, L. Shulenburg, J. T. Krogel, O. Heinonen and P. R. C. Kent, *New Journal of Physics*, 2016, **18**, 113049.
- ⁴¹J. A. Santana, J. T. Krogel, P. R. C. Kent and F. A. Reboredo, *The Journal of Chemical Physics*, 2017, **147**, year.
- ⁴²A. L. Dzubak, C. Mitra, M. Chance, S. Kuhn, J. Jellison, Gerald E., A. S. Sefat, J. T. Krogel and F. A. Reboredo, *The Journal of Chemical Physics*, 2017, **147**, year.
- ⁴³I. Kylänpää, J. Balachandran, P. Ganesh, O. Heinonen, P. R. C. Kent and J. T. Krogel, *Phys. Rev. Mater.*, 2017, **1**, 065408.
- ⁴⁴K. Saritas, J. T. Krogel, P. R. C. Kent and F. A. Reboredo, *Phys. Rev. Mater.*, 2018, **2**, 085801.
- ⁴⁵K. Saritas, J. T. Krogel and F. A. Reboredo, *Phys. Rev. B*, 2018, **98**, 155130.
- ⁴⁶K. Saritas, J. T. Krogel, S. Okamoto, H. N. Lee and F. A. Reboredo, *Phys. Rev. Mater.*, 2019, **3**, 124414.
- ⁴⁷J. A. Santana, J. T. Krogel, S. Okamoto and F. A. Reboredo, *Journal of Chemical Theory and Computation*, 2020, **16**, 643–650.
- ⁴⁸T. Ichibha, A. L. Dzubak, J. T. Krogel, V. R. Cooper and F. A. Reboredo, *Phys. Rev. Mater.*, 2021, **5**, 064006.
- ⁴⁹D. Staros, G. Hu, J. Tiihonen, R. Nanguneri, J. Krogel, M. C. Bennett, O. Heinonen, P. Ganesh and B. Rubenstein, *The Journal of Chemical Physics*, 2022, **156**, year.
- ⁵⁰M. C. Bennett, G. Hu, G. Wang, O. Heinonen, P. R. C. Kent, J. T. Krogel and P. Ganesh, *Phys. Rev. Res.*, 2022, **4**, L022005.
- ⁵¹D. Wines, J. Tiihonen, K. Saritas, J. T. Krogel and C. Ataca, *The Journal of Physical Chemistry Letters*, 2023, **14**, 3553–3560.
- ⁵²T. Zhao, Q.-L. Liu and Z.-Y. Zhao, *The Journal of Physical Chemistry C*, 2019, **123**, 14292–14302.
- ⁵³K. P. Kepp, *ChemPhysChem*, 2020, **21**, 360–369.
- ⁵⁴O. Garlea, C. Darie, C. Bougerol, O. Isnard and P. Bordet, *Solid State Sciences*, 2003, **5**, 1095–1104.
- ⁵⁵V. O. Garlea, C. Darie, O. Isnard and P. Bordet, *Solid State Sciences*, 2006, **8**, 457–461.
- ⁵⁶J.-C. Lee, Y.-W. Heo, J.-H. Lee and J.-J. Kim, *Thin Solid Films*, 2009, **518**, 1234–1237.
- ⁵⁷R. Nagarajan, N. Duan, M. Jayaraj, J. Li, K. Vanaja, A. Yokochi, A. Draeseke, J. Tate and A. Sleight, *International Journal of Inorganic Materials*, 2001, **3**, 265–270.
- ⁵⁸K. El Ataoui, J.-P. Doumerc, A. Ammar, J.-C. Grenier, P. Dordor and M. Pouchard, *Comptes Rendus Chimie*, 2004, **7**, 29–34.
- ⁵⁹I. Elsayed, M. Çavaş, R. Gupta, T. Fahmy, A. A. Al-Ghamdi and F. Yakuphanoglu, *Journal of Alloys and Compounds*, 2015, **638**, 166–171.
- ⁶⁰X. Jiang, B. Jia, D. Zhang, H. Wu, A. Chu, X. Qu and M. Qin, *Ceramics International*, 2020, **46**, 28219–28226.
- ⁶¹A. P. Mackenzie, *Reports on Progress in Physics*, 2017, **80**, 032501.
- ⁶²E. Filatov, V. Lagunova, D. Potemkin, N. Kuratieva, A. Zadesenets, P. Plyusnin, A. Gubanov and S. Korenev, *Chemistry – A European Journal*, 2020, **26**, 4341–4349.
- ⁶³G. B. Acharya, M. B. Neupane, R. Ghimire and M. P. Ghimire, *arXiv preprint arXiv:2212.00579*, 2022.
- ⁶⁴J. Shi, T. F. T. Cerqueira, W. Cui, F. Nogueira, S. Botti and M. A. L. Marques, *Scientific Reports*, 2017, **7**, 43179.
- ⁶⁵W. Wong-Ng and R. Roth, *Physica C: Superconductivity*, 1994, **233**, 97–101.
- ⁶⁶E. Lee, D. E. Brown, E. E. Alp, Y. Ren, J. Lu, J.-J. Woo and C. S. Johnson, *Chemistry of Materials*, 2015, **27**, 6755–6764.